REVIEW / SYNTHÈSE

Comparison of the multiple oligomeric structures observed for the Rvb1 and Rvb2 proteins[1]

Kevin L. Y. Cheung, Jennifer Huen, Walid A. Houry, and Joaquin Ortega

Abstract: The Rvb1 and Rvb2 proteins are 2 members of the AAA+ family, involved in roles as diverse as chromatin remodeling, transcription, small nucleolar RNA maturation, cellular transformation, signaling of apoptosis and mitosis. These proteins are capable of playing a role in such diverse cellular activities because they are components of different macromolecular assemblies. In the last few years, there has been a number of groups reporting on the structure of purified Rvbs. The reported results have been rather controversial, because there are significant differences observed among the published structures in spite of the high degree of homology among these proteins. Surprisingly, contradictions are observed not only between structures representing the Rvb proteins from different species, but also between protein structures from the same species. This review describes the available Rvb structures from different species and also makes a comparative analysis of them. Finally, we identify some aspects of these structural studies worth pursuing in additional investigations to ensure that the reported structures reflect physiologically relevant conformations of the Rvb1–Rvb2 complex.

Key words: AAA+, Rvb1, Rvb2, pontin, reptin.

Résumé : Les protéines Rvb1 et Rvb2 sont deux membres de la famille AAA+ qui jouent des rôles dans des processus aussi divers que le remodelage de la chromatine, la transcription, la maturation des petits ARN nucléoaires, la transformation cellulaire, la signalisation de l'apoptose et la mitose. Ces protéines sont capables de jouer un rôle dans ces divers processus car elles font partie de différents assemblages macromoléculaires. Au cours des dernières années, plusieurs groupes ont publié des travaux sur la structure des Rvb purifiées. Ces résultats ont été plutôt controversés car il existe des différences significatives parmi les structures publiées malgré le haut degré d'homologie parmi ces protéines. De façon surprenante, des contradictions sont observées non seulement entre les structures représentant les protéines Rvb de différentes espèces, mais aussi entre les structures protéiques déterminées au sein d'une même espèce. Cet article de revue décrit les structures disponibles de Rvb de différentes espèces et présente une analyse comparative entre elles. Finalement, nous identifions quelques aspects de ces études structurales qui mériteraient d'être davantage poussés afin de s'assurer que les structures rapportées reflètent bien les conformations pertinentes des complexes Rvb1–Rvb2.

Mots-clés : AAA+, Rvb1, Rvb2, pontine, reptine.

[Traduit par la Rédaction]

Introduction

Proteins members of the AAA+ family share similarity both in sequence and in structure (Lupas and Martin 2002; Ogura and Wilkinson 2001; Snider and Houry 2008; Snider et al. 2008). The large variety of cellular activities in which AAA+ proteins are involved (Hanson and Whiteheart 2005) was in fact the unifying theme used to name this family of proteins. AAA+ stands for "ATPases associated with diverse cellular activities" and although as a family of proteins they are involved in a large number of cellular functions, the role of each specific protein member is typically confined to a particular cellular process (Ogura and Wilkinson 2001).

The Rvb1 and Rvb2 proteins are 2 members of the AAA+ family that do not follow this pattern, as they are involved in multiple roles as diverse as chromatin remodeling, transcription, small nucleolar RNA maturation, cellular transformation, and signaling of apoptosis (Ikura et al. 2000; Shen et al. 2000). These proteins are capable of playing a role in such diverse cellular processes because they are components

Received 29 June 2009. Revision received 21 September 2009. Accepted 28 September 2009. Published on the NRC Research Press Web site at bcb.nrc.ca on 11 January 2010.

K.L.Y. Cheung and J. Ortega.[2] Department of Biochemistry and Biomedical Sciences, McMaster University, 1200 Main Street West, Hamilton, ON, L8N3Z5, Canada.
J. Huen and W.A. Houry. Department of Biochemistry, University of Toronto, Toronto, ON, M5S 1A8, Canada.

[1]This paper is one of a selection of papers published in this special issue entitled 8th International Conference on AAA Proteins and has undergone the Journal's usual peer review process.
[2]Corresponding author (e-mail: ortegaj@mcmaster.ca).

Table 1. Structural method used for determination of the Rvb protein structures.

Structure	Method for structural determination
Human Rvb1 (Matias et al. 2006)	X-ray crystallography
Human Rvb1–Rvb2 complex (Puri et al. 2007)	Negative staining electron microscopy and single particle reconstruction methods
Yeast Rvb1–Rvb2 complex (Gribun et al. 2008)	Negative staining electron microscopy and single particle reconstruction methods
Yeast Rvb1–Rvb2 complex (Torreira et al. 2008)	Cryo-electron microscopy and single particle reconstruction methods

of different macromolecular assemblies (see accompanying paper from Huen et al. 2010). In particular, the 2 proteins are found in large chromatin-remodeling complexes such as INO80 (Bakshi et al. 2006; Jin et al. 2005; Shen et al. 2000), p400 (Fuchs et al. 2001), and SWR1 (Krogan et al. 2003; Mizuguchi et al. 2004). They are also essential components of chromatin-modifying enzymes, such as the TIP60 complex, displaying histone acetylase activity. In addition, the identification of Rvb proteins in the RNA polymerase II complex (Qiu et al. 1998) and in small nucleolar ribonucleoprotein complexes (snoRNPs) (King et al. 2001; Newman et al. 2000; Zhao et al. 2008) mediates their role in transcriptional processes and nucleolar localization. Finally, the participation of the Rvb proteins in cellular transformation and apoptosis is a consequence of their interaction with c-Myc (Wood et al. 2000) and β-catenin (Bauer et al. 2000). In the last few years, the repertoire of cellular activities has been expanded even further upon the observation that these proteins are also associated to the mitotic spindle and centrosomes through a tubulin-mediated interaction (Gartner et al. 2003). These results indicate a role of these proteins in mitosis.

Given their physiological relevance, the Rvb proteins have been found to be essential in *Saccharomyces cerevisiae* (Qiu et al. 1998), *Drosophila melanogaster* (Bauer et al. 2000), and *Caenorhabditis elegans* (Matias et al. 2006), and it is likely that they are also essential in mammalian cells. Probably, the variety of cellular processes in which these proteins are involved explains the multiplicity of names given to the Rvb proteins in the literature. Rvb1 is also known as RuvBL1, Tip49a, Tip48 / Tip49, ECP-54, Pontin, Tih1, p50, and Tap54β; Rvb2 has been named RuvBL1, Tip49b, Tip49 / Tip48, ECP-51, Reptin, Tih2, p47, and Tap54α.

In the last few years, a number of groups has reported on the structure of purified Rvbs (Table 1). In 2006, the X-ray structure of a human Rvb protein (RuvBL1) assembled as a hexameric ring was reported (Matias et al. 2006). A few months later, an electron microscopy (EM) study showed the structure of a complex containing both human Rvb proteins (RuvBL1 and RuvBL2) assembled as a double hexamaric ring (Puri et al. 2007). Finally, in 2008, two independent groups published structural information regarding the complex formed by the yeast proteins Rvb1 and Rvb2 (Gribun et al. 2008; Torreira et al. 2008). The reported results have been rather controversial; in spite the high degree of homology among these proteins, there are significant differences observed among the published structures. Surprisingly, contradictions are observed not only between structures representing the Rvb proteins from different species, but also between protein structures from the same species. This review is a comparative analysis of the available structural information and proposes a number of research avenues to elucidate if the observed differences simply reflect multiple physiologically relevant functional states of these proteins or if they are caused by differences in the methodology used in the studies.

Structure of the human Rvb proteins

The X-ray structure of human Rvb1 (Matias et al. 2006) and the structure of the human Rvb1–Rvb2 complex obtained from negatively stained electron micrographs (Puri et al. 2007) were reported only a few months apart at the end of 2006 and the beginning of 2007, respectively. This section describes these two structures.

X-ray structure of the human Rvb1 protein

The X-ray structure of the human Rvb1 monomer (Matias et al. 2006) shows a protein folded into 3 domains: DI, DII, and DIII (Fig. 1A). The structure contains the typical AAA+ module that is made from domains DI and III (Fig. 1A). The first one contains the P-loop αβα nucleotide-binding core domain and consists of the typical 5-stranded β-sheet sandwiched between α-helices. The folding of DIII is also similar to many other AAA+ proteins and is formed by a bundle of α-helices. The Rvb1 protein in the structure is complexed with an ADP molecule (Fig. 1A), which provides information about how the predicted elements of the AAA+ module for nucleotide binding and hydrolysis relate to the nucleotide molecule (Fig. 1B). The conserved P-loop (Walker A motif) important for binding and orientation of the nucleotide for hydrolysis, the Walker B motif necessary for nucleotide hydrolysis, and the sensor domains (sensor 1 and 2) that also interact with the nucleotide molecule and assist in several aspects of nucleotide recognition and hydrolysis are all in a functionally compatible conformation. The Walker A and B motifs, as well as the sensor 1 domain, are located in DI, whereas the sensor 2 domain is in DIII (Fig. 1B). Superimposing the Rvb1 coordinates with those from RuvB (Putnam et al. 2001), NSF-D2 (Lenzen et al. 1998), and SV40 large tumor antigen helicase (Li et al. 2003) allowed the authors to predict the specific residues within each element of the AAA+ module involved in nucleotide binding and hydrolysis. However, a mutational analysis verifying these predictions is still not available.

In the crystal structure, the Rvb1 protein oligomerizes as a hexameric ring (Figs. 1C and 1D), which is also a hallmark of AAA+ proteins (Neuwald et al. 1999). Similarly to

Fig. 1. X-ray structure of the human Rvb1 protein. (A) Ribbon representation of the monomer of human Rvb1 in complex with an ADP molecule. Each domain is represented in a different color. (B) Closed up view of the nucleotide-binding site in the human Rvb1 structure. The elements of the AAA+ module important for nucleotide binding and hydrolysis are represented in different colors and labeled. Domains within the monomer are color coded as in A and the neighboring subunit contributing the "arginine finger" (Arg-357) is colored in grey. (C) Top-view of the ribbon representation of the hexameric ring formed by the human Rvb1 protein in the crystal structure. Each monomer is represented in a different color except the monomer at the bottom that follows the same color code as in A for the domains. (D) Side view of the ribbon representation of the human Rvb1 hexamer. The location of domains I, II, and III from the Rvb1 monomers in the hexamer is indicated. Each monomer is represented in a different color and the monomer at the front has its domains colored as in A. (E) Close-up view of the central pore in the human Rvb1 hexamer. The diameter of the pore is indicated, as well as the 2 loops within a monomer that are predicted to mediate the binding of ssDNA.

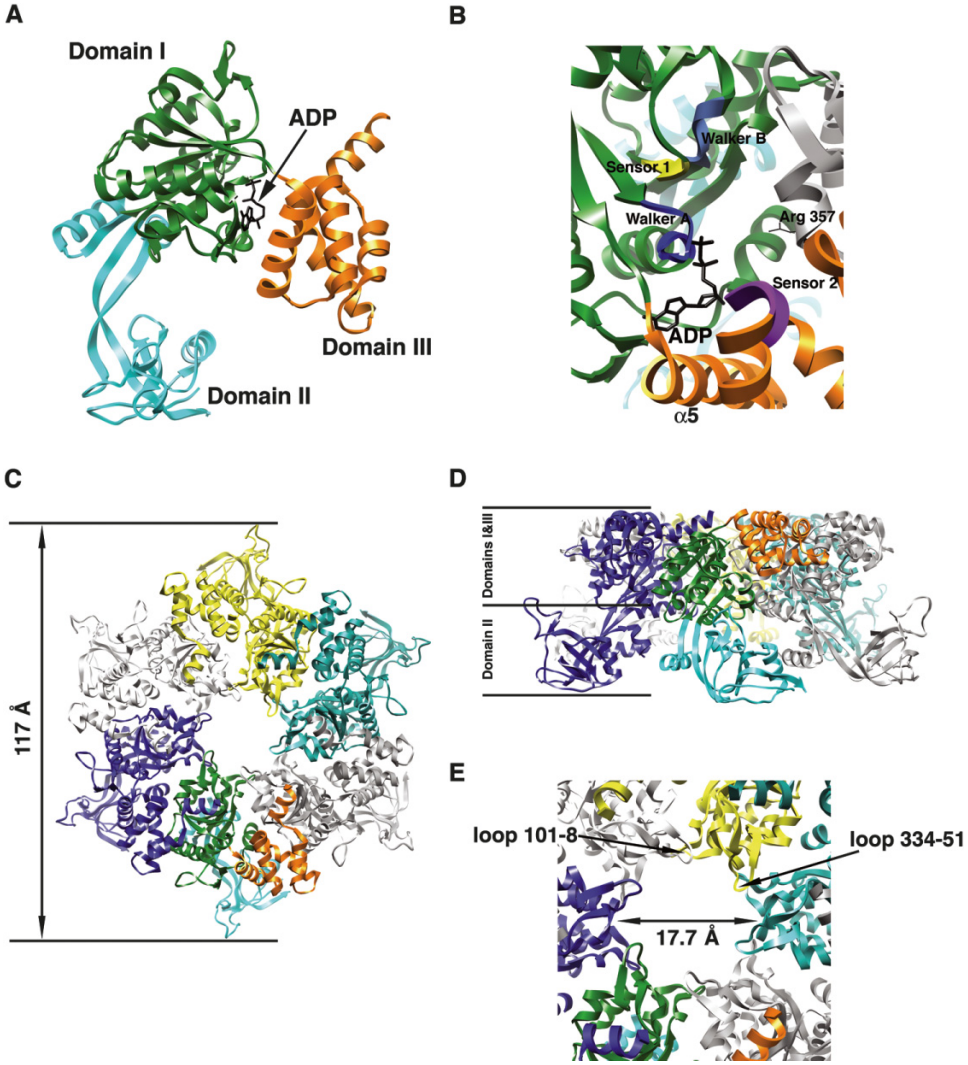

other proteins of this family, the ADP molecule was found sandwiched between two of the subunits of the ring. This particular location of the nucleotide molecule in AAA+ proteins provides the opportunity to neighboring subunits in the ring to contribute to the binding and hydrolysis of the ATP, usually through an arginine residue that contributes to nucleotide catalysis (Davey et al. 2003; Johnson and O'Donnell 2003; Karata et al. 1999; Rombel et al. 1999). In the Rvb1 protein, Arg357 in DI is close enough to the nucleotide-binding pocket of the adjacent subunit to act as the arginine finger (Fig. 1B).

An important consequence of the oligomerization of Rvb1 into a hexamer is that the ADP molecule bound to the protein becomes completely buried in the structure. One helix in DIII (α5), sensor 2, and the neighboring monomer completely block the nucleotide-binding pocket, making the release of ADP impossible (Fig. 1B), which is consistent with the lack of ATPase activity experimentally observed for human Rvb1 in the study from Matias et al. (2006). These observations support the idea that a conformational change is necessary during the nucleotide hydrolysis cycle for the ADP to ATP exchange. Interestingly, nucleotide-induced conformations have been described in the yeast Rvb1–Rvb2 complex (Gribun et al. 2008; Torreira et al. 2008). The observation that the ATPase activity of the yeast Rvb1–Rvb2 complex (Gribun et al. 2008) showed a significantly higher ATPase activity than human Rvb1 alone (Matias et al. 2006) supports the hypothesis that the presence of Rvb2 in

Fig. 2. Three-dimensional structure of the human Rvb1–Rvb2 complex obtained from negative-staining electron micrographs. (A) Surface rendering representations of the side view of the structure. Top and bottom rings are defined arbitrarily. Asterisks indicate the putative location of the DII domains. (B) Surface representation of the inside of the complex. The front half of the structure has been removed to appreciate the cavity and the channel going through the structure. (C and D) Surface representations of the 3D structure showing the top and bottom view, respectively, of the dodecameric structure.

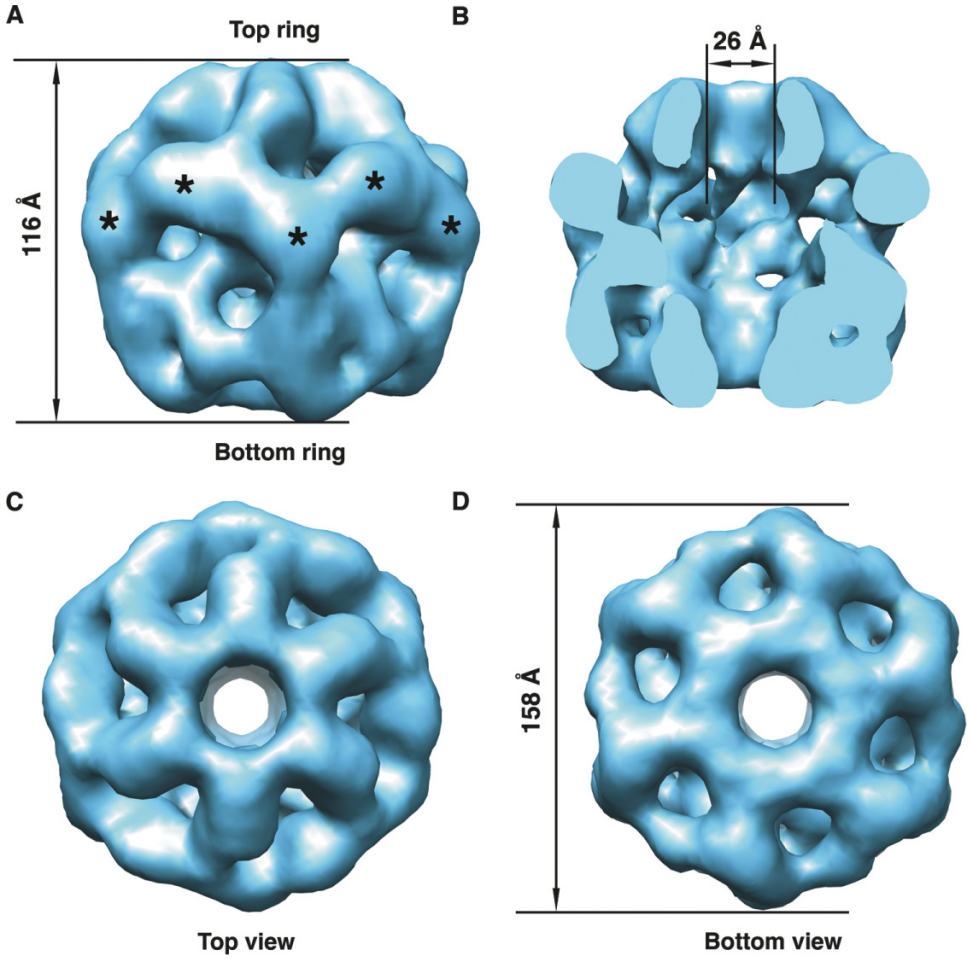

the complex is required to induce the conformational change that allows nucleotide exchange.

The Walker A and B motifs are usually closely spaced in the sequence of AAA+ proteins. However, in the Rvb proteins, there is a long insertion of ~170 amino acids between these two motifs. In the native protein, the Walker A and B motifs still come together to form the nucleotide binding site, but the 170 residue insertion domain protrudes from DI and constitutes the DII domain with an OB-fold-like structure mostly formed by β strands (Fig. 1A). The resemblance of this domain in terms of structure and surface charges to the DNA-binding domain of other proteins involved in DNA metabolism is remarkable. Matias et al. (2006) showed that human Rvb1 binding of single- (ss) and double-stranded (ds) DNA, as well as single-stranded RNA, is mediated by DII. Surprisingly, the protein was found to lack in vitro helicase activity, most likely as a consequence of its deficient ATPase activity.

Even so, this crystal structure does not explain how the interaction with nucleic acids may occur in the physiological complex, it certainly provides an initial framework to propose hypothesis for further testing. For example, it is clear that the diameter of the central channel, which is known in many hexameric AAA+ proteins as the main nucleic acid interaction site, is too narrow in the human Rvb1 hexamer (17.7 Å) for double-stranded nucleic acids to pass through (Fig. 1E). In addition, the negative electrostatic potential of the inner surface of the channel makes it better suited for binding single- rather than doubled-stranded nucleic acids, which bind to wider and positively charged channels (Fletcher et al. 2003; Li et al. 2003). Finally, there are 2 loops facing the hexameric channel (residues 101–108 and 334–351) (Fig. 1E) that resemble the ones in several hexameric AAA+ proteins, such as the T7 gp4D helicase (Singleton et al. 2000), and that were found to directly mediate the binding of ssDNA. All of these structural characteristics are consistent with the model proposed by Matias et al. (2006), suggesting that the human Rvb1 hexamer binds to forked DNA substrates. One strand of the fork will pass through the central channel, whereas the second strand will bind to the outside of the ring in an interaction mediated by the DII domain. Similarly, binding to ssRNA in transcription events could be also mediated through the central channel in the hexamer. Nonetheless, it is clear that these protein –

nucleic acid interactions are not sequence specific, indicating that they may be mediated through the sugar–phosphate backbone of the DNA and RNA. However, it is possible that other proteins in the Rvb-containing complexes might dictate certain specificity in these interactions. Additional structures of the Rvb1 protein in complex with single- and doubled-stranded nucleic acids are required to verify these interaction models.

Three-dimensional structure of the human Rvb1–Rvb2 complex by negative-staining electron microscopy

The three-dimensional (3D) reconstruction of the human Rvb1–Rvb2 complex was obtained from negatively stained electron micrographs of an in vitro assembled complex (Puri et al. 2007). Independently purified human Rvb1 and Rvb2 proteins were mixed together and the mixture was further purified and fractionated using metal affinity and size-exclusion chromatography. The fraction containing both proteins in equimolar amounts was used for the structural study.

The electron microscopy map reveals a double hexameric ring structure with a height of 116 Å (Fig. 2A) and a maximum diameter of 158 Å. The structure encloses a large cavity that opens to the outside through the axial channel running through the complex (Fig. 2B) and also through multiple small openings on the sides (Fig. 2A). The central channel is in principle wide enough (26 Å) to accommodate dsDNA (Fig. 2B). The most striking aspect of the structure is its asymmetric character, as both rings differ significantly (Figs. 2C and 2D).

The limited resolution of the structure does not allow location of the Rvb1 and Rvb2 proteins within the complex. Considering the equimolar content of Rvb1 and Rvb2 in the complex, the different structure of the two rings could indicate that each is made exclusively by one of the proteins and thus, two different homomeric rings constitute the complex. Alternatively, the structure is also consistent with a model proposing that the complex is made of two heteromeric rings of identical composition. In this case, the structural differences between rings would imply that they exist in a different conformation. Size exclusion chromatography experiments performed by Puri et al. (2007) provide some support for the homomeric rings model. It was found that Rvb2 in the presence of nucleotide (ATP or ADP) and $MgCl_2$ eluted in a peak corresponding to a molecular mass of ~400 kDa, which is slightly higher than the expected size of a Rvb2 hexamer (320 kDa). Conversely, Rvb1 always eluted as monomer regardless of the conditions tested, including in the presence of nucleotide and $MgCl_2$. The different ability of Rvb1 and Rvb2 to form stable oligomers by themselves might indicate that in the process of complex formation initially Rvb2 forms a hexameric ring that acts as a scaffold promoting the hexamerization of Rvb1 to finally render the described double hexameric ring structure. Additional experiments are required to fully establish the layout of Rvb1 and Rvb2 proteins in the dodecameric complex.

Interestingly, in the size-exclusion chromatography experiements, Puri et al. (2007) were able to assemble stable oligomers with Rvb2, but not with Rvb1; a surprising finding, given that the crystal structure of human Rvb1 suggests that it is also capable of forming higher-order oligomers. The different protein concentration used in the crystallization trials and size-exclusion chromatography experiments is probably the cause of this discrepancy.

Fig. 3. Two-dimensional structure of the yeast Rvb1–Rvb2 complex. (A) Electron micrographs of negatively stained ring-shaped particles obtained upon incubation of the Rvb1 and Rvb2 proteins in the presence of ADP. Scale bar represents 200 Å. (B) Two-dimensional averages of the yeast Rvb1–Rvb2 complex in the presence of ADP (left panel), ATP (center panel), and ATPγS (right panel). Scale bar represents 100 Å.

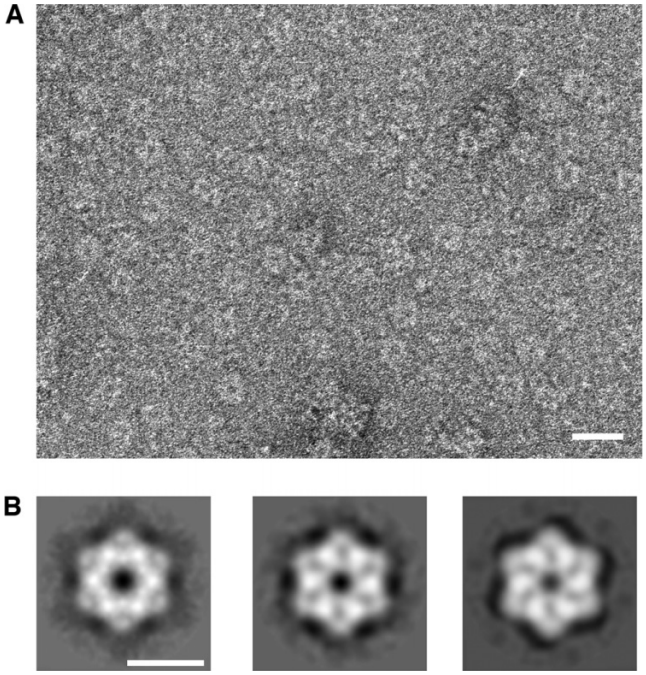

Structure of the yeast Rvb proteins

Two studies were published in the year 2008 reporting structural information about the yeast Rvb proteins (Gribun et al. 2008; Torreira et al. 2008). Both studies used electron microscopy and single-particle image-processing methods. The main highlights of the structures reported are detailed here.

Two-dimensional projection structure of the yeast Rvb1–Rvb2 complex by negative-staining electron microscopy

The first study addressing the question of the structural organization of the yeast Rvb1–Rvb2 complex was our own work using negative-staining EM and scanning transmission electron microscopy (STEM) (Gribun et al. 2008). In images obtained by STEM, the intensity at any pixel is directly proportional to the mass, providing quantitative information about the particle mass. This method was used in the study by Gribun et al. (2008) to establish that the yeast Rvb1–Rvb2 complex forms single hexameric rings. Using this method, it was determined that the distribution of masses of a large population of hexamers follows a Gaussian curve centered at the expected mass for a hexamar (~300 kDa).

Negative-staining images (Fig. 3A) were used to study the 2-dimensional (2D) structure of the complex and the conformational changes that the hexameric rings undergo in the presence of different nucleotides. Two distinct conforma-

Fig. 4. Cryo-electron microscopy 3D structure of the yeast Rvb1–Rvb2 complex. (A) Side view of the 3D structure of the Rvb1–Rvb2 complex. Top and bottom rings are indicated, as well as the location of the DI, DII, DIII, and equatorial domains of the monomers assembled within the dodecamer. The asterisks indicate the projected densities from the bottom ring into the equatorial domain. (B) The structure has been cut open to show the internal chamber, and the channel going through the structure. (C) Top view of the cryo-EM map. (D) Bottom view of the 3D EM map of the complex. The diameter of the structure is indicated.

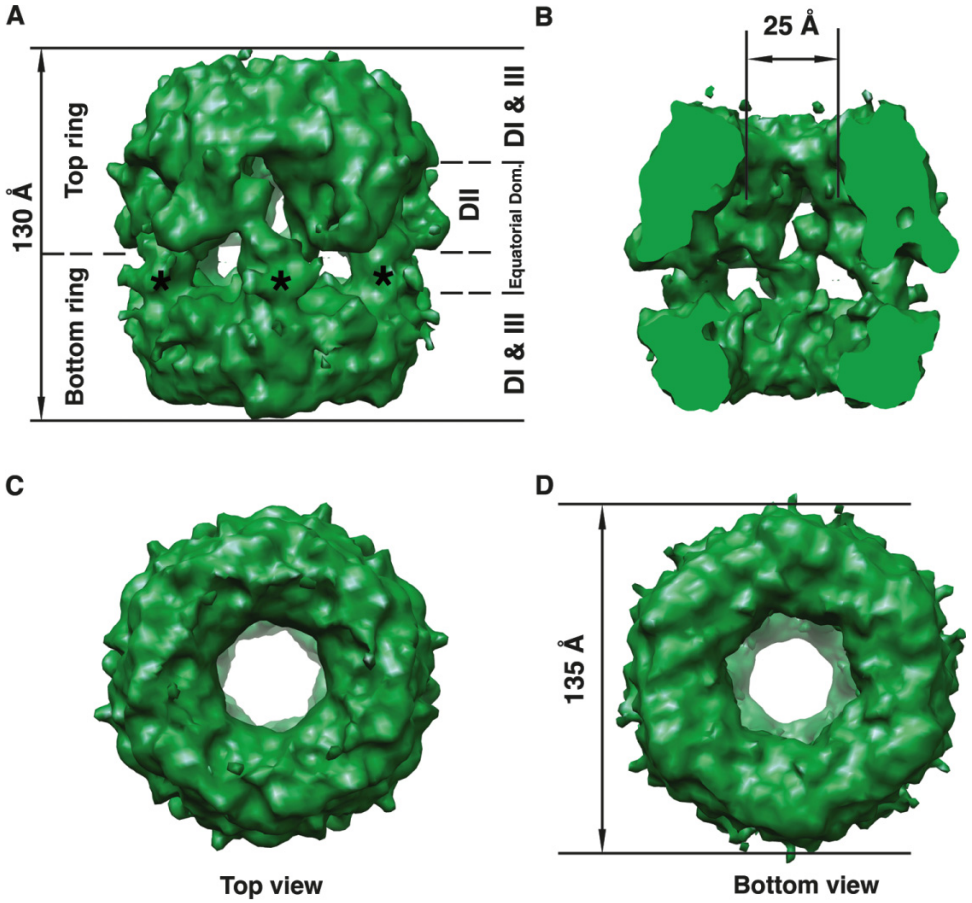

tions were identified. In the presence of ADP, the ring-shaped particles form a hexagon with straight edges measuring ~142 Å between opposite vertices and a central channel of ~17 Å diameter (Fig. 3B; left panel). The 2D projection structure of the complex in the presence of ATP (Fig. 3B, center panel) or ATPγS (Fig. 3B, right panel) showed dramatic structural differences compared with the ADP structure. In these two cases, the Rvb1–Rvb2 complex showed slightly bigger dimensions measuring ~152 Å between opposite vertices, but a smaller (~15 Å diameter) central pore. The ATP and ATPγS hexagon had concave edges and some radial areas of stain penetration instead of the smooth, stain-excluded area observed in the ADP form (Fig. 3B).

The limited resolution of the EM averages does not allow differentiating Rvb1 from Rvb2 in the 2D projection structures; thus, whether the single rings are formed by only one (homomeric) or both (heteromeric) Rvb proteins is still unclear. Our finding that both Rvb1 and Rvb2 alone form large oligomers only at very high concentrations (40 $\mu mol \cdot L^{-1}$), but that oligomers are easily formed at low concentrations (5 $\mu mol \cdot L^{-1}$) upon mixing both proteins, supports the hypothesis that the yeast Rvb1–Rvb2 complex is a single, heteromeric, hexameric ring (Gribun et al. 2008). Supporting the heteromeric model, we also found that Rvb1 and Rvb2 mixed together have an enhanced ATPase and DNA helicase activity when compared with the individual proteins (Gribun et al. 2008). Although one interpretation of these results is that homomeric rings of each protein might enhance the activity of the other by short-lived interaction in *trans*, these finding could also indicate that both the Rvb1 and Rvb2 proteins are present within the same ring and stimulation occurs in *cis*. Additional experiments reinforcing the hypothesis that the Rvb1–Rvb2 complex assembles as a heteromeric ring were the immunoprecipitation experiments performed in our study (Gribun et al. 2008). An affinity-purified αRvb1 antibody was used to immunocapture the Rvb1 protein from an equimolar mixture of Rvb1 and Rvb2. In this experiment, Rvb2 was co-immunoprecipitated with Rvb1, strongly suggesting that there is a direct interaction between the two proteins within the complex. However, it could still be argued that the interaction detected in the immunoprecipitation experiment was due to the presence of non-specific aggregates between both proteins in the incubation mixture. Certainly, further analysis is necessary to clarify this aspect of the structure of yeast Rvb1–Rvb2 complex, as well as the layout of the two proteins in the ring.

Three-dimensional structure of the yeast Rvb1–Rvb2 complex by cryo-electron microscopy

The structure of the yeast Rvb1–Rvb2 complex has also been studied by cryo-electron microscopy (Torreira et al. 2008). In this study, untagged Rvb1 was co-expressed with an N-terminal His–Rvb2 construct using recombinant baculovirus. Complexes were then purified using affinity and size-exclusion chromatography.

The purified specimen was used to produce a high-resolution 3D reconstruction of the Rvb1–Rvb2 complex (Fig. 4). According to this study, the yeast Rvb1–Rvb2 complex organizes as an asymmetric double ring structure (Fig. 4A) enclosing an internal chamber (Fig. 4B). The asymmetry is produced because the top ring (as defined in Fig. 4A) is slightly taller than the lower (Figs. 4A and B). The total height of the complex is 130 Å (Fig. 4A) and the diameter at the widest region is 135 Å (Fig. 4D). The top and bottom of the EM map are compact ring structures probably formed by DI and DIII of the Rvb proteins, where the AAA+ module is located. Six protein densities project from both the top and bottom ring towards the center of the structure, forming two layers of discontinuous density (equatorial domains) that contain lateral openings to the internal chamber of the structure (Fig. 4A). It was proposed that the DII domains that protrude from the top and bottom ring intercalate and interact in these two layers of densities in the middle of the structure to maintain the integrity of the dodecameric structure (Fig. 4A). The internal chamber is also open to the outside through an axial pore at each end of the structure. In this case, the diameter of the pore is ~25 Å, which is sufficient to accommodate dsDNA (Fig. 4B).

Interestingly, each ring in the complex displays a different conformation, mostly because of the disposition of its corresponding equatorial domain rather than the terminal ring. The projected densities from the bottom ring (Fig. 4A, asterisk) extend further than the corresponding ones in the top ring. Thus, the interactions between projections from opposite rings occur mostly in the top equatorial domain, resulting in a slightly wider layer of density with smaller lateral openings than are observed in the equatorial domain at the bottom (Fig. 4A).

The complex structurally characterized in the study by Torreira et al. (2008), contained equimolar amounts of Rvb1 and Rvb2. However, similar to the EM structure of the human Rvb1–Rvb2 complex, it was not possible to establish the layout of each protein within the complex. The 3D reconstruction of the yeast Rvb1–Rvb2 complex is equally consistent with the existence of two homomeric hexameric rings (each one formed by one of the Rvb proteins) or with an assembly formed by the stacking of two heteromeric rings containing three monomers of each protein. Antibody-labeling experiments presented in the study by Torreira et al. (2008) support the former. However, given the very low efficiency of binding reported for the antibody used in these experiments, we think this question remains unanswered.

The structure described by Torreira et al. (2008) incorporated only 34% of the particles contained in the purified Rvb1–Rvb2 complex. The remaining particles did not classify and aligned correctly during the reconstruction process to produce a double-ring structure with a different level of resolution on each ring. Rejection of 66% of the data was necessary to obtain a self-consistent data set able to produce a 3D structure. The behavior of these particles in the reconstruction process was interpreted as an indication that the Rvb1–Rvb2 complex in the sample was present in more than one conformation. A 3D reconstruction from the rejected particles was problematic and structures were not produced in the study (Torreira et al. 2008). Thus, how these other putative conformations of the yeast Rvb1–Rvb2 complex may differ from the described structure or the degree of heterogeneity in the purified complex is still unanswered.

Comparison of the Rvb structures

A problem frequently faced in structural biology is the need to compare structures at very different levels of resolution. This is the case at hand here, as some of the available structures contain atomic detail (X-ray model of Rvb1 (Matias et al. 2006)). Some others are 3D structures, but at low or moderate resolution (human (Puri et al. 2007) and yeast (Torreira et al. 2008) Rvb1–Rvb2 3D EM maps). Finally, one of the structures is only 2D and solved to a limited resolution (yeast Rvb1–Rvb2 EM average projections (Gribun et al. 2008)). However, there are several appropriate approaches to successfully compare these structures.

Relevant to the structures reviewed here are the methods used to compare X-ray structures with EM density maps. An appropriate method to perform this analysis is to fit the X-ray model into the electron density map (Rossmann 2000; Rossmann et al. 2005). When two structures are in agreement, it is found that after fitting the structures there is a corresponding electron density in the EM map for every part of the crystallographic model. In those cases where the EM structure is of limited resolution, such as the Rvb1–Rvb2 EM map analyzed here (Puri et al. 2007), the X-ray model should nicely fill the density envelope delineated by the EM structure.

It is also possible to compare atomic detail X-ray structures and high-resolution EM 3D structures to 2D projection structures of limited resolution. In this case, it is necessary to first low-pass filter the X-ray and 3D EM structure to the resolution of the 2D projection; the dimensionality of the 3D structures must then be reduced by calculating 2D projections from the 3D structures at the particular view angles represented by the 2D projection structure (Fig. 5).

Pairwise comparison between the X-ray structure of the human Rvb1 protein and the EM map of the human Rvb1–Rvb2 complex

The X-ray structure of human Rvb1 shows that it forms as a single hexameric ring in the crystal (Figs. 1C and 1D). However, the EM map represents a human Rvb1–Rvb2 complex assembled as a double hexameric ring structure (Fig. 2A). The Rvb1 single-ring X-ray structure and the observation in the size-exclusion chromatography experiments that Rvb2 assembled in stable oligomers (Puri et al. 2007) are strong indications that these proteins can assemble as single homo-oligomeric rings, suggesting that the human Rvb1–Rvb2 complex might be made of two homomeric rings. However, the question as to whether each individual

Fig. 5. Comparison of Rvb structures. To compare the available Rvb structures, high-resolution models such as human Rvb1 and yeast Rvb1–Rvb2 complex were first limited to a resolution of 25 Å by applying a Gaussian low-pass filter. A 2D projection along the 6-fold symmetry axis was calculated from the limited resolution 3D structures. In the case of the double-ring EM structure of the human and yeast Rvb1–Rvb2 complexes, independent projections were calculated for the top ("Top") and bottom ("Bottom") rings (as defined in Figs. 2 and 4). The structures are represented to scale, thus their relative size is comparable. In the case of the yeast Rvb1–Rvb2 complex from Gribun et al. (2008), the images represent 2D averages of the Rvb1–Rvb2 complex in ATP (left panel) and ATPγS (right panel) obtained by averaging several hundred 2D projections of these complexes.

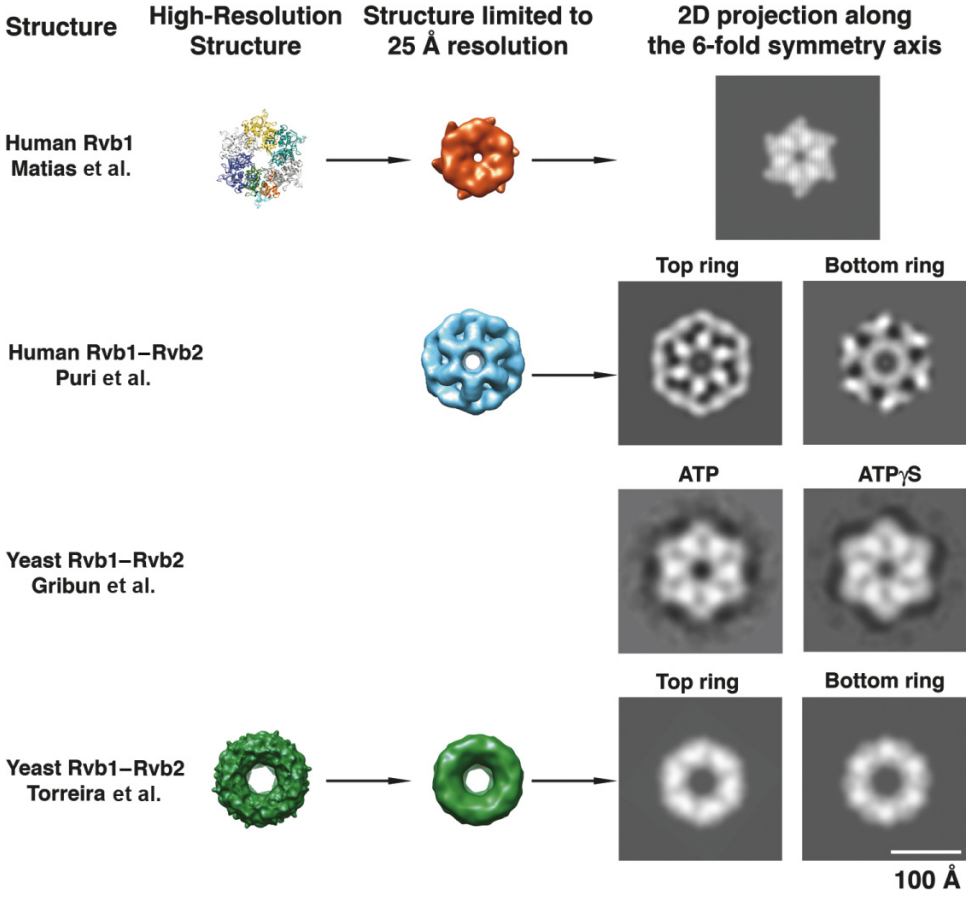

ring in the EM structure is a homomeric or heteromeric ring requires further study.

Manual docking of the X-ray structure of the Rvb1 hexamer into the EM map to analyze the agreement between structures revealed that both structures seem incompatible. The elements of the AAA+ module in the crystal structure form a compact ring between subunits with a flat top surface that contrasts with the EM structure where each ring comprises domains separated by large gaps. The observed differences are not explained by the different resolution of the structures.

An additional point of discrepancy between the structures is regarding the diameter of the central channel in the structures and the accessibility of the DII domain in the single and double ring structures. These two characteristics of the assemblies probably have important implications for how these proteins mediate their interaction with nucleic acids. The diameter and the electrostatic character of the central pore in the X-ray structure of the Rvb1 ring are consistent with ssDNA binding (Fig. 1E). However, the channel is wide enough to accommodate dsDNA in the EM structure of the Rvb1–Rvb2 complex (Fig. 2B). In the Rvb1–Rvb2 complex, DII domains are sandwiched between the two rings and their mobility is partially restricted through interactions with neighboring subunits (Fig. 2A, asterisks). Certainly, a single-ring structure, such as the hexamers formed by Rvb1, provides a less constrained and more accessible DII domain for nucleic acid interactions. Additional structures in complex with nuclei acids will clarify how the protein interacts with DNA and RNA.

Pairwise comparison between the X-ray structure of the human Rvb1 protein and the cryo-EM map of the yeast Rvb1–Rvb2 complex

The sequence identity between yeast Rvb1 and Rvb2 with human Rvb1 is of 69% and 43%, respectively. Therefore, it is expected that the X-ray structure of the human Rvb1 protein would fit well in the cryo-EM density map of the yeast Rvb1–Rvb2 complex, assuming that both structures are in a similar conformation.

Initially, Torreira et al. (2008) found that the atomic structure of the human Rvb1 hexamer fit poorly when docked as a rigid body into the ring densities at the ends of the cryo-EM map of the yeast Rvb1–Rvb2 complex. Subse-

quent rotation and outward translation of the human Rvb1 monomers within the EM density produced a good fit for the DI and DIII domains. DII domains from all 12 monomers in the complex also reasonably matched the EM densities when fitted independently from the other two domains in the equatorial region closer to the top ring in the structure (Torreira et al. 2008) (Fig. 4A). Overall, these results indicate a good agreement between the X-ray structure of the human Rvb1 protein and the yeast Rvb1–Rvb2 complex. However, the unsuccessful initial rigid body fitting of the human Rvb1 hexamer in the cryo-EM map of the yeast Rvb1–Rvb2 hexamer implies that the cryo-EM map captured a conformational state of the complex that significantly differs from the X-ray structure of the human Rvb1 protein.

As indicated, to fit the X-ray structure into the cryo-EM map, the authors had to rotate each monomer in a counterclockwise direction by approximately 5°–10°, and also displace it outwards to create a large central pore of sufficient diameter (~25 Å) to allow threading of dsDNA (Fig. 4B). A caveat of such rotational and translational movement of the Rvb monomers is that it produces a displacement of the predicted "arginine finger" that is contributed to the nucleotide-binding pocket by a neighboring subunit. Therefore, it follows that the structure of the yeast Rvb1–Rvb2 complex should undergo a conformational change from the described structure to properly place all the putative elements of the AAA+ module involved in nucleotide binding and hydrolysis.

How similar are the four available structures from human and yeast Rvb proteins?

As mentioned above, to compare structures of very different levels of detail, it is necessary to reduce the resolution and dimensionality of all structures to the lowest value of resolution and dimensions found among the compared structures. Thus, to analyze how similar the 4 structures discussed in this review are, first the resolution of the X-ray structure of human Rvb1 (Matias et al. 2006) and the EM structures of the human (Puri et al. 2007) and yeast (Torreira et al. 2008) Rvb1–Rvb2 complexes were limited to the value in the 2D projection structures of the yeast complex (Gribun et al. 2008). Next, a 2D projection was calculated from each 3D structure along their 6-fold symmetry axis. In the case of the double-ring structures (human (Puri et al. 2007) and yeast (Torreira et al. 2008) 3D reconstructions), independent projections were calculated from each ring so that structural features were not cancelled out by adding the projection of the second ring (Fig. 5). These operations reduced the resolution and dimensionality of the 3D structures and it was possible to make a comparison with the 2D average projection of the yeast Rvb1–Rvb2 complex.

The comparison of the 2D projections from human and yeast structures showed certain similarities between the crystal structure of human Rvb1 (Matias et al. 2006) and both yeast structures (Gribun et al. 2008; Torreira et al. 2008) (Fig. 5). This is consistent with the docking experiments of Torreira et al. (2008) that showed good agreement between the cryo-EM map of the yeast Rvb1–Rvb2 complex and the X-ray structure of the human Rvb1 hexamer. The differences observed between the 2D projections generated from both structures, mainly the larger central pore in the yeast structure, are not surprising given the rotation and outward translations applied to the monomers in the human Rvb1 hexamer to fit the EM density of the yeast Rvb1–Rvb2 structure (Torreira et al. 2008). We also notice that the projections obtained from the cryo-EM structure of the yeast complex (Torreira et al. 2008) were more rounded than the projection structures obtained by us (Gribun et al. 2008), and the one obtained from the X-ray structure of the human Rvb1 (Matias et al. 2006) had a hexagonal shape with concave edges. According to the crystal structure of the human Rvb1 hexamer, the DII domains constitute the vertices of the hexamer. These domains in the double-ring structure of the yeast complex (Torreira et al. 2008) extend downward, interacting in the equatorial domain and locking their position rather than protruding outward. The different conformation of the DII domains in the cryo-EM map of the yeast complex (Torreira et al. 2008) explains the more rounded shape of the projections obtained from this structure.

As mentioned, the projection from the X-ray structure of human Rvb1 (Matias et al. 2006) had commonalities with the negatively stained EM average projections of the yeast Rvb1–Rvb2 complex (Gribun et al. 2008) in the ATP or ATPγS conformation (Fig. 5), but not with the projection of the complex in the presence of ADP (Fig. 3). This is surprising, as the X-ray structure of the human Rvb1 reveals that the protein in this structure is complexed with ADP. In addition, we also noticed that the hexameric rings formed by the yeast Rvb1–Rvb2 complex obtained by negative-staining electron microscopy (Gribun et al. 2008) are significantly bigger than the ring formed by human Rvb1 (Matias et al. 2006), but they have similar dimensions to the cryo-EM reconstruction of the yeast complex (Torreira et al. 2008) (Fig. 5). There is no obvious reason at this point to explain the observed difference in size between the X-ray and EM structures.

Consistent with the incompatibility of the X-ray structure of human Rvb1 (Matias et al. 2006) and the EM reconstruction of the human complex (Puri et al. 2007) derived from the docking experiment performed with these two structures, the projections obtained from the human Rvb complex were very dissimilar to the projections obtained from all the other structures, including the X-ray structure of human Rvb1 (Matias et al. 2006) (Fig. 5).

All in all, a conclusion that can be obtained from this comparison is that in spite of the double- or single-ring structure adopted by these proteins in the different structures, there is a reasonable degree of compatibility between three of the structures (X-ray structure of the human Rvb1 (Matias et al. 2006) and the two EM structures of the yeast complex (Gribun et al. 2008; Torreira et al. 2008). Probably, the EM reconstruction of the human Rvb1–Rvb2 complex (Puri et al. 2007), which is incompatible with the other structures, captures the assembly in a somehow unique conformation.

Roadmap to elucidate the physiologically relevant structures and conformational changes of the Rvb1–Rvb2 complexes

The human Rvb1 and Rvb2 proteins share 40% sequence

Table 2. Buffer conditions.

Structure	Buffer conditions	Nucleotide bound
Human Rvb1 (Matias et al. 2006)	20 mmol·L^{-1} Tris–HCl, pH 8.0, 150 mmol·L^{-1} NaCl, 10% glycerol, 1 mmol·L^{-1} dithiothreitol	ADP
Human Rvb1–Rvb2 complex (Puri et al. 2007)	20 mmol·L^{-1} Tris–HCl, pH 8.0, 100 mmol·L^{-1} NaCl, 10% glycerol, 1 mmol·L^{-1} PMSF, 1 mmol·L^{-1} dithiothreitol, 1 mmol·L^{-1} EDTA	No nucleotide added
Yeast Rvb1–Rvb2 complex (Gribun et al. 2008)	25 mmol·L^{-1} Tris–HCl, pH 7.5, 200 mmol·L^{-1} KCl, 10% glycerol, 1 mmol·L^{-1} dithiothreitol	ADP, ATP and ATPγS
Yeast Rvb1–Rvb2 complex (Torreira et al. 2008)	25 mmol·L^{-1} Tris–HCl, pH 8.0, 125 mmol·L^{-1} NaCl	No nucleotide added

Table 3. Protein constructs and expression methods.

Structure	Construct, assembly	Expression system
Human Rvb1 (Matias et al. 2006)	N-His-FLAG Rvb1	*E.coli* BL21 (DE3)
Human Rvb1–Rvb2 complex (Puri et al. 2007)	Rvb1–Rvb2-His-C, in vitro	*E.coli* BL21 (DE3)
Yeast Rvb1–Rvb2 complex (Gribun et al. 2008)	Rvb1–Rvb2, in vitro	*E.coli* BL21 (DE3)
Yeast Rvb1–Rvb2 complex (Torreira et al. 2008)	Rvb1–N-His-Rvb2, in vivo	Baculovirus

identity. In addition, there is also a high degree of identity between the yeast and human Rvb proteins. Therefore, it is expected that these proteins share a high degree of structural similarity. Consistently, we found a reasonable degree of structural similarity between three of the structures. However, it is surprising that both the human and yeast Rvb proteins were found forming single- and double-ring oligomers. Certainly, it is possible that these proteins undergo conformational changes while performing their diverse functions or upon nucleotide hydrolysis. It is also possible that a single-ring structure is required to perform certain aspects of their functionality, but a double-ring complex may be necessary for others. Thus, the solved structures may simply represent different functional states. However, careful analysis of the details of these studies during the elaboration of this review red flagged some aspect of these studies worth pursuing for additional analysis to ensure that the reported structures reflect relevant physiological conformational states of the Rvb1–Rvb2 complex.

Differences such as the buffer conditions and the presence or absence of nucleotides in the current structures could be triggering these structural differences (Table 2). However, a first point of concern is the use of differently tagged versions of the Rvb proteins in some of the studies (Table 3). Only in the study from Gribun et al. (2008) was the Rvb1–Rvb2 complex assembled from untagged proteins. In this study, proteins were expressed as N terminal His tag proteins. However, the tag was removed before the assembly of the complex as performed. Also, in the study from Torreira et al. (2008), although the majority of the structural characterization was done in an Rvb1 – N terminal His Rvb2, it was reported (Torreira et al. 2008) that the complex still remained as a double-ring structure after the His tag was removed immediately after complex assembly. Results obtained in our laboratory have shown that an N terminal His tag attached to either yeast Rvb1 or Rvb2 promotes the assembly of a double rather than a single hexameric structure[3]. Additional structures produced from untagged Rvb proteins are essential at this point to rule out the possibility that the tags may be inducing non-physiological conformational and oligomeric states.

Furthermore, several systems were used in the different structures to overexpress the protein constructs (Table 3). These ranged from bacterial to insect cell-based expression system. Also, in some cases the complexes were assembled in vitro from purified components, and in others they were obtained in vivo through co-expression of both proteins. It is certainly a concern how human or yeast proteins expressed in bacterial systems, as well as the Rvb1–Rvb2 complexes assembled in vitro, relate to the native complexes. In this case, purification and structural analysis of the endogenous complexes will provide important insights on the effect of the expression and assembly system in the structure of the complex.

Once the effects of protein tags, expression system, and in vitro vs. in vivo assembly on the structure has been studied or to some ruled out, it will be beneficial to perform the structure determination of these complexes at conditions close to physiological conditions, or under those conditions where ATPase and helicase activity have been observed. Analysis of the structures in the apo-form, but also bound to nucleotides and ultimately to nucleic acids, will certainly unveil physiologically relevant structures and conformations of the Rvb1–Rvb2 complex.

In addition, whether the hexameric rings formed by these proteins are homomeric or heteromeric, as well as the stoichiometry and layout of Rvb1 and Rvb2 proteins in the complex, remain a major unsolved issue. In the absence of a crystal structure of the human or yeast Rvb1–Rvb2 complex, this is one question where electron microscopy can contribute great insights through protein-labeling experiments.

[3] K.L.Y. Cheung, J. Huen, W.A. Houry, and J. Ortega. Alternative oligomeric states of the yeast Rvb1–Rvb2 complex induced by histidine tags. Manuscript in preparation.

Finally, as our knowledge expands on the protein partners of the Rvb proteins in multiple macromolecular assemblies (see accompanying manuscript from Huen et al. 2010) where these proteins are found, the next challenge will be to determine the structure of these larger assemblies to eventually understand the physiological role of Rvb proteins in the broader context of large macromolecular complexes.

Acknowledgements

Images were produced using the UCSF Chimera package from the Resource for Biocomputing, Visualization, and Informatics at the University of California, San Francisco (supported by NIH P41 RR-01081). Our work in this field is supported by a Discovery grant from the National Science and Engineering Research Council of Canada (J.O), the National Cancer Institute of Canada (W.A.H., number 016372), and the Canadian Institutes of Health Research (W.A.H., MOP-93778). J.O. is Canadian Institutes of Health Research New Investigator.

References

Bakshi, R., Mehta, A.K., Sharma, R., Maiti, S., Pasha, S., and Brahmachari, V. 2006. Characterization of a human SWI2/SNF2 like protein hINO80: demonstration of catalytic and DNA binding activity. Biochem. Biophys. Res. Commun. **339**(1): 313–320. doi:10.1016/j.bbrc.2005.10.206. PMID:16298340.

Bauer, A., Chauvet, S., Huber, O., Usseglio, F., Rothbächer, U., Aragnol, D., et al. 2000. Pontin52 and reptin52 function as antagonistic regulators of beta-catenin signalling activity. EMBO J. **19**(22): 6121–6130. doi:10.1093/emboj/19.22.6121. PMID:11080158.

Davey, M.J., Indiani, C., and O'Donnell, M. 2003. Reconstitution of the Mcm2-7p heterohexamer, subunit arrangement, and ATP site architecture. J. Biol. Chem. **278**(7): 4491–4499. doi:10.1074/jbc.M210511200. PMID:12480933.

Fletcher, R.J., Bishop, B.E., Leon, R.P., Sclafani, R.A., Ogata, C.M., and Chen, X.S. 2003. The structure and function of MCM from archaeal M. Thermoautotrophicum. Nat. Struct. Biol. **10**(3): 160–167. doi:10.1038/nsb893. PMID:12548282.

Fuchs, M., Gerber, J., Drapkin, R., Sif, S., Ikura, T., Ogryzko, V., et al. 2001. The p400 complex is an essential E1A transformation target. Cell, **106**(3): 297–307. doi:10.1016/S0092-8674(01)00450-0. PMID:11509179.

Gartner, W., Rossbacher, J., Zierhut, B., Daneva, T., Base, W., Weissel, M., et al. 2003. The ATP-dependent helicase RUVBL1/TIP49a associates with tubulin during mitosis. Cell Motil. Cytoskeleton, **56**(2): 79–93. doi:10.1002/cm.10136. PMID:14506706.

Gribun, A., Cheung, K.L., Huen, J., Ortega, J., and Houry, W.A. 2008. Yeast Rvb1 and Rvb2 are ATP-dependent DNA helicases that form a heterohexameric complex. J. Mol. Biol. **376**(5): 1320–1333. doi:10.1016/j.jmb.2007.12.049. PMID:18234224.

Hanson, P.I., and Whiteheart, S.W. 2005. AAA+ proteins: have engine, will work. Nat. Rev. Mol. Cell Biol. **6**(7): 519–529. doi:10.1038/nrm1684. PMID:16072036.

Huen, J., Kakihara, Y., Ugwu, F., Cheung, K., Ortega, J., and Houry, W.A. 2010. Rvb1/2: essential ATP-dependent hilcases for critical complexes. Biochem. Cell. Biol. **88**: this issue.

Ikura, T., Ogryzko, V.V., Grigoriev, M., Groisman, R., Wang, J., Horikoshi, M., et al. 2000. Involvement of the TIP60 histone acetylase complex in DNA repair and apoptosis. Cell, **102**(4): 463–473. doi:10.1016/S0092-8674(00)00051-9. PMID:10966108.

Jin, J., Cai, Y., Yao, T., Gottschalk, A.J., Florens, L., Swanson, S.K., et al. 2005. A mammalian chromatin remodeling complex with similarities to the yeast INO80 complex. J. Biol. Chem. **280**(50): 41207–41212. doi:10.1074/jbc.M509128200. PMID:16230350.

Johnson, A., and O'Donnell, M. 2003. Ordered ATP hydrolysis in the gamma complex clamp loader AAA+ machine. J. Biol. Chem. **278**(16): 14406–14413. doi:10.1074/jbc.M212708200. PMID:12582167.

Karata, K., Inagawa, T., Wilkinson, A.J., Tatsuta, T., and Ogura, T. 1999. Dissecting the role of a conserved motif (the second region of homology) in the AAA family of ATPases. Site-directed mutagenesis of the ATP-dependent protease FtsH. J. Biol. Chem. **274**(37): 26225–26232. doi:10.1074/jbc.274.37.26225. PMID:10473576.

King, T.H., Decatur, W.A., Bertrand, E., Maxwell, E.S., and Fournier, M.J. 2001. A well-connected and conserved nucleoplasmic helicase is required for production of box C/D and H/ACA snoRNAs and localization of snoRNP proteins. Mol. Cell. Biol. **21**(22): 7731–7746. doi:10.1128/MCB.21.22.7731-7746.2001. PMID:11604509.

Krogan, N.J., Keogh, M.C., Datta, N., Sawa, C., Ryan, O.W., Ding, H., et al. 2003. A Snf2 family ATPase complex required for recruitment of the histone H2A variant Htz1. Mol. Cell, **12**(6): 1565–1576. doi:10.1016/S1097-2765(03)00497-0. PMID:14690608.

Lenzen, C.U., Steinmann, D., Whiteheart, S.W., and Weis, W.I. 1998. Crystal structure of the hexamerization domain of N-ethylmaleimide-sensitive fusion protein. Cell, **94**(4): 525–536. doi:10.1016/S0092-8674(00)81593-7. PMID:9727495.

Li, D., Zhao, R., Lilyestrom, W., Gai, D., Zhang, R., DeCaprio, J.A., et al. 2003. Structure of the replicative helicase of the oncoprotein SV40 large tumour antigen. Nature, **423**(6939): 512–518. doi:10.1038/nature01691. PMID:12774115.

Lupas, A.N., and Martin, J. 2002. AAA proteins. Curr. Opin. Struct. Biol. **12**(6): 746–753. doi:10.1016/S0959-440X(02)00388-3. PMID:12504679.

Matias, P.M., Gorynia, S., Donner, P., and Carrondo, M.A. 2006. Crystal structure of the human AAA+ protein RuvBL1. J. Biol. Chem. **281**(50): 38918–38929. doi:10.1074/jbc.M605625200. PMID:17060327.

Mizuguchi, G., Shen, X., Landry, J., Wu, W.H., Sen, S., and Wu, C. 2004. ATP-driven exchange of histone H2AZ variant catalyzed by SWR1 chromatin remodeling complex. Science, **303**(5656): 343–348. doi:10.1126/science.1090701. PMID:14645854.

Neuwald, A.F., Aravind, L., Spouge, J.L., and Koonin, E.V. 1999. AAA+: A class of chaperone-like ATPases associated with the assembly, operation, and disassembly of protein complexes. Genome Res. **9**(1): 27–43. PMID:9927482.

Newman, D.R., Kuhn, J.F., Shanab, G.M., and Maxwell, E.S. 2000. Box C/D snoRNA-associated proteins: two pairs of evolutionarily ancient proteins and possible links to replication and transcription. RNA, **6**(6): 861–879. doi:10.1017/S1355838200992446. PMID:10864044.

Ogura, T., and Wilkinson, A.J. 2001. AAA+ superfamily ATPases: common structure-diverse function. Genes Cells, **6**(7): 575–597. doi:10.1046/j.1365-2443.2001.00447.x. PMID:11473577.

Puri, T., Wendler, P., Sigala, B., Saibil, H., and Tsaneva, I.R. 2007. Dodecameric structure and ATPase activity of the human TIP48/TIP49 complex. J. Mol. Biol. **366**(1): 179–192. doi:10.1016/j.jmb.2006.11.030. PMID:17157868.

Putnam, C.D., Clancy, S.B., Tsuruta, H., Gonzalez, S., Wetmur, J.G., and Tainer, J.A. 2001. Structure and mechanism of the RuvB Holliday junction branch migration motor. J. Mol. Biol. **311**(2): 297–310. doi:10.1006/jmbi.2001.4852. PMID:11478862.

Qiu, X.B., Lin, Y.L., Thome, K.C., Pian, P., Schlegel, B.P., Weremowicz, S., et al. 1998. An eukaryotic RuvB-like protein (RUVBL1) essential for growth. J. Biol. Chem. **273**(43): 27786–27793. doi:10.1074/jbc.273.43.27786. PMID:9774387.

Rombel, I., Peters-Wendisch, P., Mesecar, A., Thorgeirsson, T., Shin, Y.K., and Kustu, S. 1999. MgATP binding and hydrolysis determinants of NtrC, a bacterial enhancer-binding protein. J. Bacteriol. **181**(15): 4628–4638. PMID:10419963.

Rossmann, M.G. 2000. Fitting atomic models into electron-microscopy maps. Acta Crystallogr. D Biol. Crystallogr. **56**(Pt 10): 1341–1349. doi:10.1107/S0907444900009562. PMID:10998631.

Rossmann, M.G., Morais, M.C., Leiman, P.G., and Zhang, W. 2005. Combining X-ray crystallography and electron microscopy. Structure, **13**(3): 355–362. doi:10.1016/j.str.2005.01.005. PMID:15766536.

Shen, X., Mizuguchi, G., Hamiche, A., and Wu, C. 2000. A chromatin remodelling complex involved in transcription and DNA processing. Nature, **406**(6795): 541–544. doi:10.1038/35020123. PMID:10952318.

Singleton, M.R., Sawaya, M.R., Ellenberger, T., and Wigley, D.B. 2000. Crystal structure of T7 gene 4 ring helicase indicates a mechanism for sequential hydrolysis of nucleotides. Cell, **101**(6): 589–600. doi:10.1016/S0092-8674(00)80871-5. PMID:10892646.

Snider, J., and Houry, W.A. 2008. AAA+ proteins: diversity in function, similarity in structure. Biochem. Soc. Trans. **36**(Pt 1): 72–77. doi:10.1042/BST0360072. PMID:18208389.

Snider, J., Thibault, G., and Houry, W.A. 2008. The AAA+ superfamily of functionally diverse proteins. Genome Biol. **9**(4): 216. doi:10.1186/gb-2008-9-4-216. PMID:18466635.

Torreira, E., Jha, S., López-Blanco, J.R., Arias-Palomo, E., Chacón, P., Cañas, C., et al. 2008. Architecture of the pontin/reptin complex, essential in the assembly of several macromolecular complexes. Structure, **16**(10): 1511–1520. doi:10.1016/j.str.2008.08.009. PMID:18940606.

Wood, M.A., McMahon, S.B., and Cole, M.D. 2000. An ATPase/helicase complex is an essential cofactor for oncogenic transformation by c-Myc. Mol. Cell, **5**(2): 321–330. doi:10.1016/S1097-2765(00)80427-X. PMID:10882073.

Zhao, R., Kakihara, Y., Gribun, A., Huen, J., Yang, G., Khanna, M., et al. 2008. Molecular chaperone Hsp90 stabilizes Pih1/Nop17 to maintain R2TP complex activity that regulates snoRNA accumulation. J. Cell Biol. **180**(3): 563–578. doi:10.1083/jcb.200709061. PMID:18268103.